J Nanopart Res (2012) 14:688
DOI 10.1007/s11051-011-0688-1

RESEARCH PAPER

In situ thermolysis of magnetic nanoparticles using non-hydrated iron oleate complex

Meng Meng Lin · Do Kyung Kim

Received: 9 September 2011 / Accepted: 22 December 2011 / Published online: 26 January 2012

Abstract A novel strategy for the fabrication of nanostructured materials based on preparation of metallic surfactants is presented and some examples are demonstrated in this article. The suggested synthetic procedure of metal oleate is universal, potentially able to produce bulk quantities, and can be applicable to the synthesis of other metal oxide and metal nanoparticles. In general, organometallic compounds are quite expensive and are mostly classified as a highly toxic substance. In this study, we used simple, inexpensive, and eco-friendly approaches to prepare the metallic surfactants. As an example, non-hydrated iron oleate (FeOl) complexes are prepared as precursors for the in situ-fabricated superparamagnetic iron oxide nanoparticles (SPIONs) by thermolysis. The different coordination of the non-hydrated FeOl complexes are directly relating to the competition between nucleation and crystal growth. The in situ preparation of SPIONs involves the reaction of metal nitrate and carboxylic acid at 120 °C to synthesize the non-hydrated FeOl complexes and following the thermolysis of FeOl at 300 °C in non-coordination solvent. The coordination modes and distinct thermal behaviors of intermediates non-hydrated FeOl complexes are comparatively investigated by means of thermo-analytic techniques complimented by differential scanning calorimetry, thermal gravimetric analysis (TGA) and infrared spectroscopy (FTIR). The potential chemical structures of non-hydrated FeOl and their reaction mechanism by thermolysis were elucidated. The resulting lipid-coated SPIONs were characterized by transmission electron microscope, FTIR, differential temperature analysis, and TGA. These data suggested a bimodal interaction of organic shell and nanoparticle surface, with chemically absorbed inner layer and physically absorbed outer layer of carboxylic acid.

Keywords Superparamagnetic · Iron oxide · SPIONs · Iron oleate · Monodispersed · Thermolysis · Ferrofluids · Metallic surfactants · Nanomaterials fabrication

Electronic supplementary material The online version of this article (doi:10.1007/s11051-011-0688-1) contains supplementary material, which is available to authorized users.

M. M. Lin
Department of Chemical Engineering, Tsinghua University, Yingshi Building, Beijing, China

D. K. Kim (✉)
Department of Biomedical Science, Jungwon University, Goesan 367-805, South Korea
e-mail: eurokorean@gmail.com; dokyung@jwu.ac.kr

Introduction

The nanocrystalline magnetic particles are intensively used as ferrofluid because of their remarkable new physiochemical properties such as superparamagnetism and their potential for broad applications in

storage disk, bulletproof armor, magnetic sealing/break, transformer coolant, oscillation damping, magnetic ink, magneto-fluorescent, biomedical, nanocomposite, etc. Over the last two decades, properly surface-modified superparamagnetic iron oxide nanoparticles (SPIONs) had been intensively investigated in both fundamental scientific research and healthcare, such as MR contrast agents (Feng et al. 2011; Yeh et al. 2010; Jeon et al. 2009), drug delivery system (DDS) (Kim and Dobson 2009), magnetic tracking for diagnosis (Wang et al. 2003) of disease, and cancer hyperthermia (Lee et al. 2011; Simioni et al. 2011). The unique physiochemical properties, i.e., high field irreversibility, monodispersibility, colloidal stability, finite size, geometric shapes, and high saturation field in the range of superparamagnetism, i.e., smaller than 20 nm, of SPIONs are crucial factors for high value-added applications (Deng et al. 2005). Recently, several synthetic strategies have been attempted to develop the process for monodispersed colloidal magnetic nanoparticles consisting of unique SPIONs in both size and shape. In general, the synthetic schemes could be classified based on aqueous or non-aqueous routes, and each individual technique possesses contrasting properties directly reflecting on their ultimate applications. Aqueous-based coprecipitation technique is a straightforward, facile, and economic process, but frequently associated with high degree of agglomeration, broad size distribution, which results in loss of superparamagnetism, increased overall cost, and decreased yield (Li et al. 2005). Although relatively superior dispersion and controllable size distribution can be achieved by microemulsion, it associates with unpleasant obstacles such as environmental issues caused by waste and difficulties of removing excessive surfactant.

Recently, inspired by process and techniques that would yield high-quality monodispersed nanocrystals, the thermal decomposition of organometallic precursors is intensively developed to fabricate highly monodispersed metal oxide nanocrystals consisting of uniform size and morphologies. In this approach, the distinctive physicochemical properties are exclusively tunable because of the complete separation of nucleation and particle growth. Hyeon et al. reported monodispersed γ-Fe_2O_3 nanocrystals by thermal decomposition of iron pentacarbonyl in the presence of oleic acid (OA) as surfactant and octyl ether as solvent (Hyeon et al. 2001). Sun et al. demonstrated successful synthesis of magnetite nanoparticles under 265 °C by thermal decomposition of iron acetoacetonate as iron precursors in the presence of phenyl ether, OA, oleylamine, and 1,2-hexadecanediol (Sun and Zeng 2002). Hyeon also reported inexpensive and eco-friendly organometallic iron precursor iron (FeOl) by ion exchange of iron chloride and sodium oleate salts and effectively synthesized high quality SPIONs in large scale (Park et al. 2004). The merit of FeOl complexes as an iron precursor by thermal decomposition is that SPIONs with wide range of sizes can be obtained by varying reaction conditions; therefore, research has been directed to focus on economic and effective synthesis of FeOl resulting in highly monodispersed nanocrystals with tunable size. Currently, two synthetic methods are available to prepare hydrated FeOl: reacting of iron chloride and sodium oleate at equimolar amounts in water and oil interface, and dissolution of iron hydroxide in oleic acid (Park et al. 2004); however, both processes are associated with inevitable problems. In the reaction between iron chloride and sodium oleate, separate purification steps for removing by-products of sodium salts from hydrolysis of sodium oleate are compulsory, and therefore, it is complicated, time-consuming work, and the measurement of FeOl yield are crucial, while dissimilar probability of metal coordination is presented (Bronstein et al. 2007). In this process, water interference of the FeOl complex through hydrogen bond cannot be avoided and may cause catastrophic vapor explosion together with vigorous spraying of hot oil in glass condenser and inhomogeneous heating subsequently at extreme thermolysis temperature. Moreover, some authors have reported that FeOl can exist as both mononuclear and polynuclear structures. The partial dissolution of goethite in carboxylic acid is frequently taking place, and the optimizations of Fe/OA ratios are still under investigation for monodispersed SPIONs with a tunable particle size (Yu et al. 2004). Bronstein et al. studied the influence of FeOl structure on iron oxide nucleation and particle growth (Bronstein et al. 2007). Kwon et al. reported the reaction kinetics of SPION's formation via thermal decomposition of FeOl complex by thermal gravimetric mass spectrometric (TG-MS) analysis, and a simulation model was proposed to elucidate the reaction mechanism (Kwon et al. 2007).

Although some pioneering studies are explored to optimize the ratio of Fe/carboxylic acid and possible

reaction mechanisms, the accurate stoichiometric composition is not fully understood. It has been reported that the by-product H_2 could serve as a reducing agent from Fe^{3+} to Fe^{2+} in Fe_3O_4 (Kwon et al. 2007). Moreover, the stoichiometric ratio of Fe/OA, which is directly relating to the chemical structures and reaction mechanisms, is too complex to be controlled because the various amounts of oleic acid are formed during the hydrolysis of sodium oleate.

In conventional process for hydrated FeOl, several steps are involved including purifications and drying process in freeze dryer. Especially, the FeOl is difficult to handle because of the tacky solid state with a high viscosity. Thus, the FeOl used in master batch production is usually provided in the form of an organic solvent, e.g., in a 50% solution in hydrocarbon. Their tar-like properties hinder the preparation of stoichiometric composition of precursors to tune the particle sizes of SPIONs.

In this article, we describe simple technique to synthesize non-hydrated FeOl complexes by coordination of metal ion and carboxylic acid, i.e., direct interaction of equimolar iron nitrate and oleic acid, in which the by-product HNO_3 could serve as a catalyst. Although excess surfactants such as oleylamine are known to act as capping agents for good morphology and controlling the particle's size, oleylamine is not involved in the process for investigating the influence of metal coordination with carboxylic acid on the formation of particles. Especially, when fatty-amine is used as a surfactant; washing out of the excess chemicals on the surface of the particles becomes very difficult to handle. Moreover, further conjugation with biomolecules such as protein and peptide is impossible. In this report, the straightforward and eco-friendly routes for SPIONs are developed by thermolysis of non-hydrated FeOl followed by aging at nucleation temperature. The chemical structures of non-hydrated FeOl complexes are further characterized with respect to frequencies of vibrations between bonds of atoms, and the reaction mechanisms are investigated by heat flow on physiochemical transformation, i.e., phase transition, thermal behaviors during thermal decomposition, nucleation, and particle growth mechanisms. We also examined the structural influence and nucleation mechanism of SPIONs depending on different coordination modes of non-hydrated FeOl and hydrated FeOl.

Experimental procedure

Iron (III) chloride hexahydrate ($FeCl_3 \cdot 6H_2O$, 98.0%), Iron (III) nitrate nonahydrate ($Fe(NO_3)_3 \cdot 9H_2O$, 97.0%), *cis*-9-octadecenoic acid (OA, 90.0%), hexane (99.0%), ethanol (95%), 1-octadecene (ODE, 90.0%) were obtained from Sigma-Aldrich. All the chemicals were used without further purification except ODE. Volatile substances such as absorbed water and organic impurities with a low Mw in ODE were evaporated by heating at 200 °C for 3 h before use. Double-distilled and deionized water was used throughout. Non-hydrated FeOl complexes produced by direct coordination of carboxylic acid to metal ions at elevated temperature. In brief, 0.404 g of $Fe(NO_3)_3$ $9H_2O$ was first mixed with desired amount of OA (see Table 1) in three-neck round-bottom flask. Lab-built PID temperature controller was directly connected to heating mantle. The mixture was heated to 120 °C to remove the physically absorbed water and by-product, HNO_3. During the reaction, mixture color changes to dark red brownish from the orange. The temperature of the reactants was decreased to room temperature and collected for analysis. By increasing the amount of oleic acid, the non-hydrated FeOl tends to be more tacky solids; FeOl-NODW14 and FeOl-NOMW15 are viscous reddish brown phase. For comparison, hydrated FeOl complexes were also prepared with $FeCl_3 \cdot 6H_2O$ and sodium oleate as starting materials in the mixture of hexane, ethanol, and water as solvent. The sample notation and preparation methods are described in Table 1. The 1 mmol (0.404 g) of $Fe(NO_3)_3$ $9H_2O$ and proper amount (4–8 mmol) of OA, and 5 mL of ODE were dissolved in three-neck round-bottom flask. For example, the sample notation of "N1453" means "Nanoparticles, 1 mmol of Fe source, 4 mmol of OA, 5 mL of ODE, and 30 min of reaction time." The sample notation of "FeOl-NODW14" means "Iron oleate prepared with 1 mmol iron nitrate and 4 mmol of OA." Lab-built PID temperature controller was directly connected to heating mantle. The mixture was heated to 120 °C for 1 h to evaporate the physically absorbed water and HNO_3. After 30 min, air condenser was connected for refluxing. The reaction mixture was then heated to 320 °C for 30 min with a heating rate of 3.3 °C/min under magnetic stirring resulting in the reddish brown solution being turned into black. The lipid-coated SPIONs were dissolved in 5 mL hexane, precipitated

by 10 mL ethanol, and centrifuged at 14,000 rpm for 10 min, and the supernatant was carefully decanted. The washing process repeated for five times, and the lipophilic magnetic nanoparticles were re-dispersed in 5 mL hexane, forming a stable magnetic fluid and kept at 4 °C for further used for characterization and applications. Fourier transform infrared (FTIR) spectra were recorded at 20 °C using ALPHA FT-IR spectrometers equipped with platinum ATR (single reflection diamond ATR) from Bruker optics. The spectra were measured with a resolution of 1 cm^{-1}, and the wavenumber range was 650–4,000 cm^{-1}. The samples were measured by dropping the samples on the surface of facet of diamond ATR without any specific preparation of specimens. Thermal gravimetric analysis (TGA), differential scanning calorimetry (DSC), and differential thermal analysis (DTA) analysis were carried out using Q600 simultaneous DSC–DTA–TGA system from TA Instruments. The Q600 system was controlled by Thermal Advantage and Universal Analysis software for data acquisition and analysis. In data plots, the weight loss is expressed as a percentage of the initial sample weight and plotted versus temperature. DSC and DTA with nitrogen purge gas (20 mL/min) were used to heat samples (5–10 mg) in platinum pans with pierced lids (TA Instruments). Samples were measured from 20 to 400 °C at a nominal heating rate of 10 °C/min.

Results and discussion

Non-hydrated FeOl complex were advantageously prepared by coordination of a trivalent inorganic salts and carboxylic acid (RCOOH) with various molar ratios at 120 °C. The trivalent metal ion can be introduced in any of various forms, but in particular, a trivalent inorganic metal salt (such as a nitrate) is introduced because trivalent iron could effect more coordination than divalent iron. These multivalent transition metal cations and particularly Fe(III), which are essentially capable of coordinating RCOOH, include those having 10 to 22 carbon atoms. Carboxyl acid groups in monobasic carboxylic acid are ionized by neutralization with metal ions caused by their strong metal cation chelating ability. A typical reaction equation for non-hydrated FeOl complex is described as follows:

$$\mathrm{Fe(NO_3)_3 + 3CH_3(CH_2)_7CH{=}CH(CH_2)_7COOH \rightarrow Fe(C_{17}H_{33}COO)_3 + 3HNO_3\uparrow} \quad (1)$$

The synthetic procedure for non-hydrated FeOl has several following advantages. First, by-product HNO_3 is served as a catalyst for the coordination resulting in high degree of conversion of organometallic complexes. In general, excess alcohol and organic/inorganic acid were suggested to increase the reactivity of carboxylic acid and metal ions. The non-hydrated FeOl as an organometallic precursor is more reasonable than hydrated FeOl to synthesize SPIONs by thermolysis, while immiscible water molecules will not interrupt the thermal decomposition in non-coordination solvent. The particles sizes of SPIONs are tuned by equimolar ratios of metal ion and carboxylic acid without excessive passivating surfactant/solvent. Especially, the molecular structures of non-hydrated FeOl complexes are strongly correlated to molar ratios of Fe/OA, the correlation of coordination modes; thermal behaviors of non-hydrated FeOl and their particle formation are investigated.

In this manner, the suggested process can be more generalized. For the formation of magnetic nanoparticles: Iron salt (i.e., $FeCl_2$, $FeCl_3$, and

Table 1 Sample notation and composition of FeOl

Sample notation	Iron source (C, N)	Surfactant (S, O)	Solvent (M, D)	Washing method (W, E)
FeOl-CSMW	$FeCl_3{\cdot}6H_2O$	Na oleate	Mixture of hexane, IMS and water	None
FeOl-CSME	$FeCl_3{\cdot}6H_2O$	Na oleate		Ethanol
FeOl-NOMW	$Fe(NO_3){\cdot}9H_2O$	Oleic acid		None
FeOl-NODW1X (X = 1,2,3,4,5)	$Fe(NO_3){\cdot}9H_2O$	Oleic acid	None	None

In sample notation *C* means iron chloride, *N* means iron nitrate, *S* means sodium oleate, *O* means oleic acid, *M* means mixture of solvents, *D* means direct reaction without solvent, *W* means without washing process, and *E* means ethanol washing process

$Fe(NO_3)_3{\cdot}9H_2O$, $FeSO_4{\cdot}4H_2O$) in the form of hydrous/nonhydrous, depending on whether it is possible to dissolve in alcohol or not. Any carboxylic acids, such as oleic acid, linoleic acid, steric acid, and lauric acid, could be used as metal coordinating substances. The merit of this process is that the stoichiometric composition can be easily prepared. For example, when 1 mol of $FeCl_3$ was used, 3 mol of oleic acid was added. Preferably, alcohol can be added at concentrations 10 times those of the carboxylic acid (vol %) if metal salt is not directly dissolved in carboxylic acid. The sample is heated at 120 °C for 30 min to evaporate the alcohol. It is to be remembered that hydrated metal oleate will form when alcohol is involved. After preparing the viscous waxy iron oleate, the sample can be easily dissolved in the organic solvents (such as 1-hexadecene, octyl ether 1-octadecene, 1-eicosene, or trioctylamine). This procedure could involve application of more complicated metal salt forms. If metal salts are difficult to dissolve in alcohol, then aqua regia or strong acid (HCl or HNO_3) are suggested to dissolve them. In this case, drying process is essential by freeze drying over night.

The molecular structures and thermal behaviors of non-hydrated FeOl and hydrated FeOl complexes were determined by FTIR, DSC, TGA, and DTA. Figure 1a) shows FT-IR spectra of oleic acid and non-hydrated FeOl and hydrated FeOl complexes prepared with different compositions. In FeOl-NODW14 spectrum, two $-CH_2$ bands at 2,925 and 2,852 cm^{-1} located at the same position as in OA, and there appears a small shoulder at 2,958 cm^{-1}, which can be assigned to asymmetrical $-CH_3$ vibration mode, whereas, OA spectrum is hard to distinguish because of strong $\nu_a(-CH_2)$ at 2,925 cm^{-1} (Mahajan and Dikerson 2007; Shukla et al. 2003) (See supplementary information.). In the region of 1,600–1,500 cm^{-1}, several new peaks were identified as metal carboxylate bands according to Bronstein's study: three bands at 1,588, 1,552, and 1,524 cm^{-1} were assigned to asymmetrical carboxylate vibration, whereas the strong band appearing at 1,436 cm^{-1} was assigned to symmetrical vibration. In Fig. 1, a major peak appears at 1,709 cm^{-1}, which can be assigned as C=O stretching band of OA or asymmetrical vibration of unidentate mode (Shukla et al. 2003). The intensity of the band at 1,709 cm^{-1} increases linearly with increasing amount of OA. The coordination modes of FeOl complexes were determined based on the position and separation of asymmetrical and symmetrical iron carboxylate peaks, and splitting amount, Δ (Bronstein et al. 2007). Four types of metal

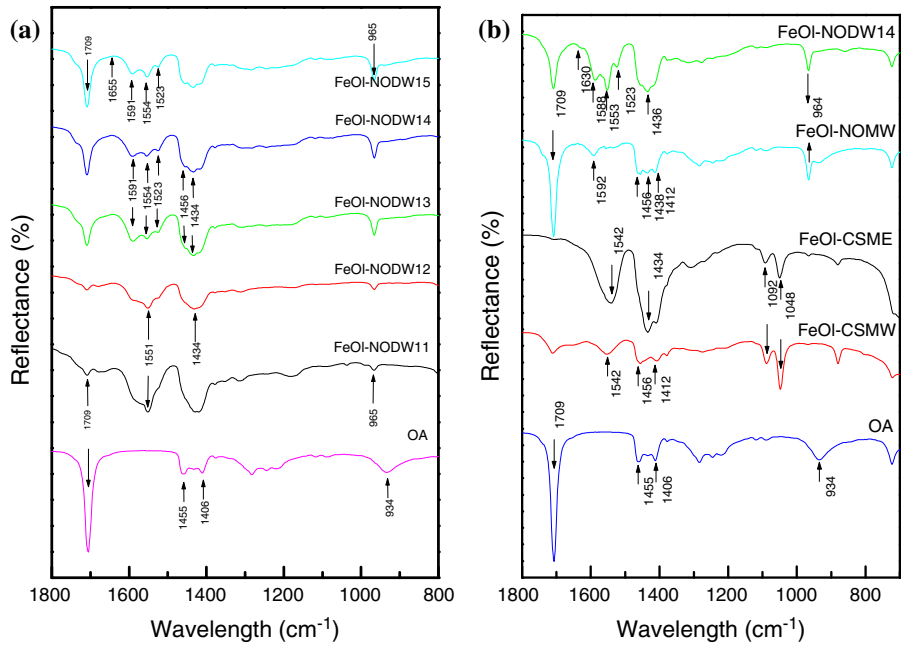

Fig. 1 FTIR spectra of **a** oleic acid, FeOl-CSMW, FeOl-CSME, FeOl-NOMW, and FeOl-NODW14, **b** non-hydrated FeOl prepared with different molar ratios of metal ion and oleic acid (FeOl-NODW11–FeOl-NODW15)

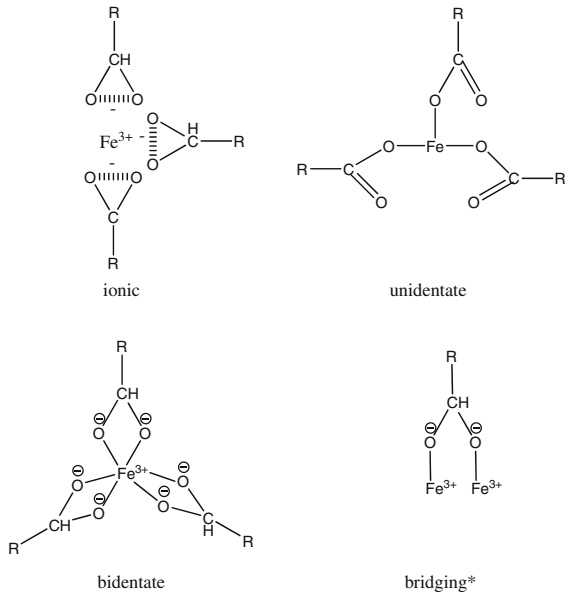

Scheme 1 Four coordination modes of iron carboxylate: ionic, unidentate, bidentate, and bridging. * The other two valents are not shown in the scheme for simplicity

carboxylate coordination modes were described in Scheme 1: ionic, unidentate, bidentate, and bridging mode. For $\Delta > 200$ cm^{-1}, unidentate mode can be expected; for $110 < \Delta < 200$ cm^{-1}, it is a bridging mode; and for $\Delta < 110$ cm^{-1}, it is a bidentate mode (Bronstein et al. 2007). For FeOl-NODW14, the differences between characteristic bands within $\nu(COO^-)$ region are 152, 118, and 88 cm^{-}1, revealing bridging and bidentate modes.

The FTIR spectra of hydrated FeOl-CSMW and FeOl-CSME complexes (prepared by Hyeon's method, before and after washing with ethanol, respectively) and their structural influences of hydroxyl group by washing with ethanol are investigated in Fig. 1a). In FeOl-CSMW, a broad band at $\sim$3,400 cm^{-1} (data not shown) and a strong band at 1,709 cm^{-1} are due to –OH stretching and C=O stretching of unreacted OA, respectively, and three peaks located at 2,958, 2,925, and 2,852 cm^{-1} are assigned to $\nu_a(-CH_3)$, $\nu_a(-CH_2)$, and $\nu_s(-CH_2)$, respectively.(Park et al. 2004; Mahajan and Dikerson 2007) The absence of bands at 3,400 and 1,709 cm^{-1} in FeOl-CSME spectrum is due to complete removal of liberated OA molecules by washing with ethanol. In FeOl-CSMW, the peak at 1,552 cm^{-1} is assigned to $\nu_a(COO^-)$, whereas 1,455 and 1,406 cm^{-1} are corresponding to $\nu_s(COO^-)$. In FeOl-CSME, the new symmetrical carboxylate vibration bands that appeared at 1,434 cm^{-1}, 1,455, and 1,406 cm^{-1} bands have disappeared, giving a $\Delta = 118$ cm^{-1} indicating purely bridging coordination. Interestingly, in non-hydrated FeOl complexes, symmetrical iron carboxylate vibration band appears at 1,436 cm^{-1} without washing with ethanol. To investigate the effect of different solvents on FeOl complexes structures, FTIR spectra of non-hydrated FeOl-NODW14 and hydrated FeOl-NOMW are compared. In $\nu(COO^-)$ region of FeOl-NOMW IR spectrum, there are characteristic iron carboxylate bands appearing at 1,592, 1,456, 1,438, and 1,412 cm^{-1}, giving rise to $\Delta = 136$, 154, and 180 cm^{-1}, respectively, all belonging to bridging coordination mode. However, in FeOl-NODW14, apart from the peak at 1,588 cm^{-1}, two new peaks corresponding to asymmetrical vibration appear at 1,553 and 1,523 cm^{-1}, and only one strong band at 1,436 cm^{-1} which is assigned to symmetrical vibration. The different splitting (Δ) is due to the slightly different structure formed. With hydrated FeOl complex, a mixture of hexane, ethanol, and water is employed as solvent; the water in the mixture interferes with the reaction and forms hydrogen bond to the complex, and the water droplets formed by thermolysis repeatedly lead to a catastrophic vapor explosion together with inhomogeneous heating because of the large latent heat of vaporization of water molecules resulting in agglomeration of particles. In contrast, with non-hydrated metal oleate complexes as starting materials, no water molecules are involved in molecular structures, and the possibility of interference with hydrated molecules are drastically minimized. The molecular structures of hydrated FeOl-NOMW were proposed in Bronstein's study, where OA molecules exist as dimers and bind to Fe ion through both unidentate and bidentate modes, whereas water molecules are attached to iron ion via hydrogen bond (Bronstein et al. 2007). To compare the difference of molecular structures between hydrated FeOl and non-hydrated FeOl, we investigated the most feasible molecular structures of non-hydrated FeOl prepared in this report. Iron ions bind to dimeric oleate ligands in both bidentate and bridging modes without water molecules or ethanol molecule, as shown in Scheme 2.

The structural influences of different amounts of OA are investigated during the formation of

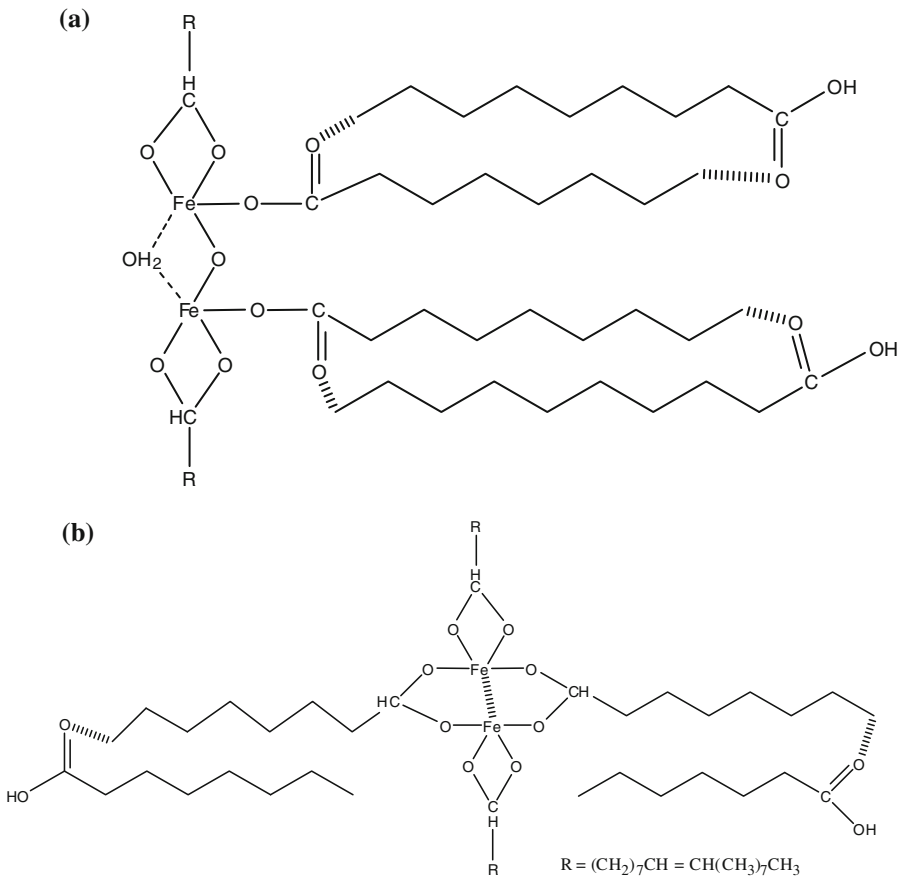

Scheme 2 Structure of iron oleate complex: **a** hydrated iron oleate complex and **b** non-hydrated iron oleate

non-hydrated FeOl complexes. Figure 1b shows FTIR spectra of non-hydrated FeOl complexes prepared by varying the molar ratios of $Fe(NO_3)_3$ and OA from 1/1 to 1/5. Compared to pure OA, several new peaks appear in the region of 1,650–1,500 cm^{-1} in all non-hydrated FeOl samples because of the newly formed iron carboxylate, and a strong peak appearing at 1,434 cm^{-1} is also assigned to carboxylate vibration. The bands at 1,591, 1,554, and 1,523 cm^{-1} are assigned to $v_a(COO^-)$ of non-hydrated FeOl complexes, among which the band at 1,554 cm^{-1} has the strongest intensity. The very small peak at 1,655 cm^{-1}, which appeared in FeOl-NODW15, can be assigned to C=C stretching mode, indicating that the double bond structure is intact in non-hydrated FeOl complexes. However, in FeOl-NODW11 to FeOl-NODW14, this peak was too weak to be detectable. The intensity of characteristic unreacted OA band at 1,709 cm^{-1} had increased with decreasing ratio of $Fe(NO_3)_3$ and OA, with FeOl-NODW15 displaying the strongest intensity of 1,709 cm^{-1} band, which could be explained by increasing amount of solid dimerized unreacted OA. In FeOl-NODW11 and FeOl-NODW12, distinguished peaks appeared at 1,551 and 1,436 cm^{-1}, which can be assigned to asymmetrical and symmetrical carboxylate vibrations, respectively, giving raise a $\Delta = 115$ cm^{-1} indicating that only bridging mode exists in these FeOl complexes. With increased OA concentration in FeOl complexes preparation, additional asymmetrical carboxylate vibration bands appeared at 1,591 and 1523 cm^{-1}, resulting in new values for $\Delta = 165$ and 87 cm^{-1}. Therefore, in FeOl-NODW13, FeOl-NODW14, and FeOl-NODW15, the carboxylate heads bind to iron atom in both bidentate and bridging modes.

Transmission electron microscope images of samples N1153–N1553 prepared with varying Fe/OA molar ratios in starting reaction mixture are shown in Fig. 2a–e. By varying molar ratios of Fe/OA from 1:1 to 1:5, the diameter of resulted nanocrystallites can be tuned at fixed reaction temperature (320 °C) and time

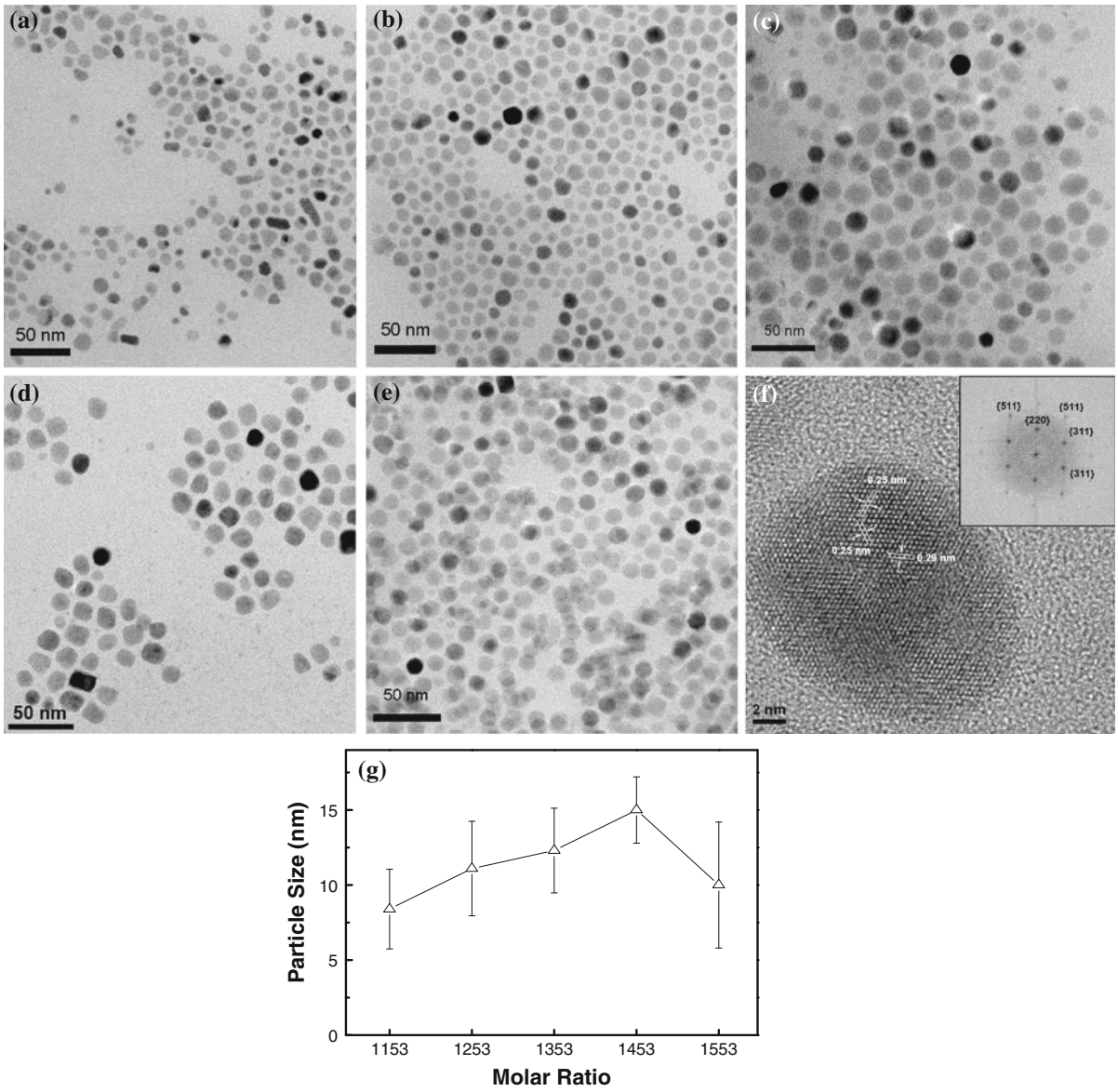

Fig. 2 **a–e** TEM images of N1153, N1253, N1353, N1453, and N1553 prepared by thermal decomposition at 320 °C for 30 min in ODE **f** HRTEM image of N1453 and **g** the variation of magnetic particle size depending on molar ratio (indicated by sample numbers) of metal ion and oleic acid

(30 min). When molar ratio of 1:1 (N1153) was employed, the sample has different morphologies, such as triangle, cubic, spherical, and irregular shapes (Fig. 2a). With increasing OA concentration, not only the size of iron oxide nanocrystals was increased, but also the morphology of particles tend to be uniform as hexagonal in N1253 and N1353, cubic in N1453, and spherical in N1553. High-resolution TEM analysis showed that nanoparticles in all the samples were highly crystalline. Figure 2f shows a crystalline nanoparticle from sample N1453, with the most intense lattice fringes being observed from the {220} to {311} planes (Fig. 2f inset). The average diameters of the nanoparticles in samples N1153–N1553 were calculated to be 8.4, 11.1, 12.3, 15, and 10 nm, respectively (Fig. 2g). Interestingly, the particle size increases by increasing the OA molar ratio from 1:1 to 1:4. However, the particle size started to decrease

when OA molar ratio is raised to 1:5. In sample N1553, spherical nanocrystals of 10-nm diameter were obtained without any size selection process; therefore, the particles were practically monodispersed. During the particle formation, lower amounts of carboxyl acid against metal irons will form irregular shape and size. The particle size linearly increases when OA is used in the ratio up to 1:4; thereafter, the particle size will start to decrease. When free OA is present during the reaction, the free carboxylate acid will attack the surface of nucleated particles as a reverse reaction and bind to iron atoms, and start to leach out as an iron oleate. The spherical shapes of the particles are formed mainly because it is thermodynamically stabler than other morphologies in this reaction condition. However, when the reaction time was prolonged further, different morphologies start to appear with an irregular crystal growth. Because the chemical structure of carboxylic acid will decompose under the presence of magnetic nanoparticles which will serve as catalysis. To summarize, small amount of carboxylic acid will enhance the nucleation of nanoparticles. Optimal amount of carboxylic acid will produce monodispersed nanoparticles. However, prolonged reaction time will cause the decomposition of carboxylic acid (FeOl) resulting in large size with irregular morphologies.

Successful synthesis of monodispersed SPIONs strongly relies on the complete separation of nucleation and crystal growth. In the case of thermolysis of hydrated FeOl, the nucleation initiates from generation of thermally free radicals of metal carboxylate (Yu et al. 2004) as follows:

$$\mathrm{M-COOR} \xrightarrow{320\ ^\circ\mathrm{C}} \mathrm{M^\bullet} + \mathrm{RCOO^\bullet} \quad (2)$$

$$\mathrm{M-COOR} \xrightarrow{320\ ^\circ\mathrm{C}} \mathrm{M-O^\bullet} + \mathrm{RC^\bullet O} \quad (3)$$

The generated free radicals may recombine to each other or get decomposed to volatile molecules such as CO, CO_2, H_2O, ester, etc. Mainly free radicals attack other M–COOR molecules to trigger the chain reaction; therefore, a burst of nucleation is generated followed by slow nucleation using FeOl as precursor. Carboxylic acid plays two roles in the synthesis of iron oxide nanocrystals: first, the carboxylate functional group of OA binds to the iron species to form iron oleate (FeOl) complexes as the iron precursors; second, free oleic acid serves as capping agent to prevent particle aggregation, and therefore, a perfect dispersion in organic solvents, such as hexane, toluene, and chloroform, can be obtained. Participation of oxidizing agent is also essential for the formation of SPIONs; some authors employed mild oxidizing agents, such as trimethylamine oxide, to avoid the formation of undesired wüsitite structure ($Fe_{1-x}O$, where $0.05 < x < 0.17$). Casula had produced monodispersed magnetite with multiple injections of oxidizing agents and polydispersed mixture of magnetite and wüsitite with a single injection of oxidizer (Casula et al. 2006). In this study, air was kept purged thoroughly through the reaction mixture as a sufficient oxygen supply for formation of magnetite and maghemite. It is also possible that metastable wüsitite was transformed to a mixture of α-Fe and magnetite, and surface-accumulated α-Fe was oxidized to magnetite when exposed to air (Casula et al. 2006).

The non-hydrated FeOl complexes in different ratios of $Fe(NO_3)_3$ and OA and without any washing process are subjected to thermal analysis. The pure OA is also subjected to thermal analysis to investigate its thermal behaviors for comparison with non-hydrated FeOl complexes. There is a distinguished exothermic peak at 266 °C indicating decomposition of free OA, which is in good agreement with the literature (Roca et al. 2006). The one set temperature of thermal decomposition of free OA is 231 °C as shown in TGA of OA (see supplementary information), and the weight percentage decreased to 11% when the temperature reached 267 °C, indicating that the majority of OA has been decomposed to CO, CO_2, H_2O, H_2, ketones, esters, and hydrocarbons with different chain lengths (Kwon et al. 2007), while the mass percentage is decreased to 0% at 600 °C indicating complete decomposition of OA.

The solid waxy forms of non-hydrated FeOl complexes are subjected to thermal analysis to enable us study the reaction mechanism of nanoparticles formation. Based on FTIR data, non-hydrated FeOl samples are a mixture of unreacted OA and FeOl with different coordination modes. According to Bronstein, the first transition appears at 132 °C in crude hydrated FeOl sample because of removal of chemically absorbed water (Bronstein et al. 2007), whereas no such endothermic peak appeared in non-hydrated FeOl. The absence of this endothermic peak is supplementary evidence supporting the prediction of FTIR analysis that no water molecules are involved in the synthesized non-hydrated FeOl complexes. As

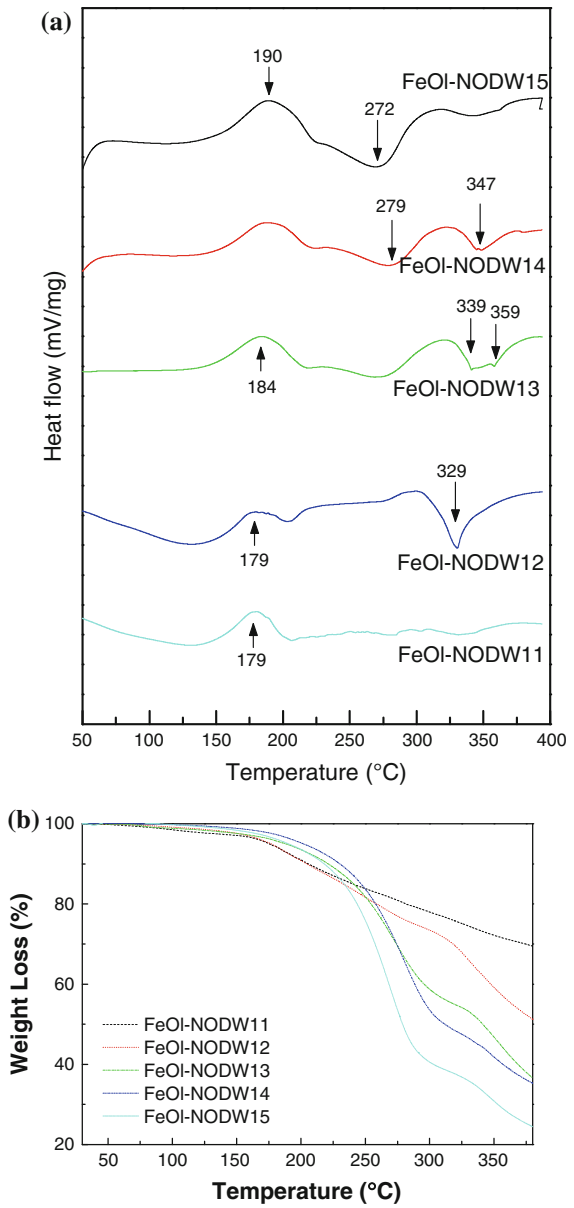

Fig. 3 **a** DSC curves and **b** TGA curves of non-hydrated FeOl prepared with different molar ratio of metal ion and oleic acid (FeOl-NODW11–FeOl-NODW15)

shown in Fig. 3a, the first endothermic peak of non-hydrated FeOl complexes appeared at 179–190 °C in all samples, which is assigned to the initiation of dissociation of oleate ligand and nucleation of SPIONs. With increasing ratio of OA against iron ions, the endothermic peak was right shifted, indicating stronger association of oleate ligand and iron atom. The TGA curves show a good agreement with the endothermic peak in Fig. 3b. In non-hydrated FeOl-NODW14 complexes, for example, the on-set temperature of the first weight loss is determined to be 190 °C, and the resulting weight loss from 191 to 241 °C is 8.1%. The second transition appears, at around 270–280 °C in DSC curves of FeOl samples, as a shallow exothermic peak. According to Bronstein and Heyon (Hyeon et al. 2001; Bronstein et al. 2007), the peak near 300 °C can be assigned to the dissociation of the remaining oleate ligands from hydrated FeOl precursors which lead to particle growth. Interestingly, the thermal decomposition temperature of OA was determined to be 266 °C, and obviously therefore coordination with iron had stabilized the oleate molecules and increased the decomposition/dissociation temperatures of OA. In the non-hydrated FeOl complexes, the OA amount is increased from FeOl-NODW11 to FeOl-NODW15, which matches the fact that the second exothermic transition peaks increased from 270 to 285 °C. The second exothermic transition peaks match the second-step weight loss from 241 to 299 °C, as seen in TGA curve of FeOl-NODW14 in Fig. 3b. The weight loss of the second step is 39.4%; thus, it is reasonable to conclude that the first weight loss is due to removal of free OA and dissociation of one oleate ligand, while the second weight loss from 331 to 400 °C is due to dissociation of the remaining two oleate ligands. The significant separation of second and third thermal transition peaks of FeOl-NODW14 and FeOl-NODW15 (175–190 °C) is a clear indication of complete separation of nucleation and particle growth phases and, hence, production of highly monodispersed SPIONs. However, the second transition peak around 270 °C in FeOl-NODW11 is also undetectable indicating that nucleation and particle growth happen at the same time at 330 °C; therefore, polydispersed particle is expected for FeOl-NODW11. Bronstein et al. has assigned the peak at 380 °C to complete thermal decomposition of hydrated FeOl (Bronstein et al. 2007). However, this exothermic peak is due to the oxidation of previously formed SPIONs ~330 °C, as it is well known that magnetite is easily oxidized into maghemite under high temperature. No significant weight increase is observed in TGA curves at this temperature either; this could be explained by the fact that the weight losses of organic compounds are faster than weight gains because of oxidation. In FeOl-NODW14, the remaining weight percentage was

34.6%, which can be considered as due to the formation of iron oxides.

SPIONs prepared by thermolysis of non-hydrated FeOl-NODW14 are denoted as N1453. FTIR spectra of SPIONs were recorded and comparison is shown in Fig. 4. In Sample N1153–N1553, two bands appearing at 1,737 and 1,711 cm^{-1} were assigned to C=O stretching bands of monomer and dimer OA, respectively (Shukla et al. 2003). The absence of 1,737 cm^{-1} in N1153 and N1253 spectra indicate the lack of monomeric OA in these samples, and therefore, the concentration of OA does have an influence on interaction between coated OA and iron oxide surface. No significant C=C stretching of OA can be distinguished at 1,656 cm^{-1}, probably because of interfacing by the 1,711 cm^{-1} peak (Roca et al. 2006). In samples N1153–N1353, there is a band at 1,554 cm^{-1} assigned to asymmetrical carboxylate vibration, whereas in N1453 and N1553, the band is broadened, possibly because it splits to two peaks at 1,588 and 1,552 cm^{-1} (Mahajan and Dikerson 2007; Shukla et al. 2003). The 1,464 cm^{-1} band appearing in samples N1153–N1553 is assigned to symmetrical carboxylate vibration. An intense peak appeared at 588 cm^{-1} in N1153 and N1253, because of Fe–O bonding; however, this peak is quiet weak to allow distinguishing in the rest of samples, caused by the full coverage of OA on the surface.

Differential temperature analysis and TGA were employed to study the thermal behaviors of the

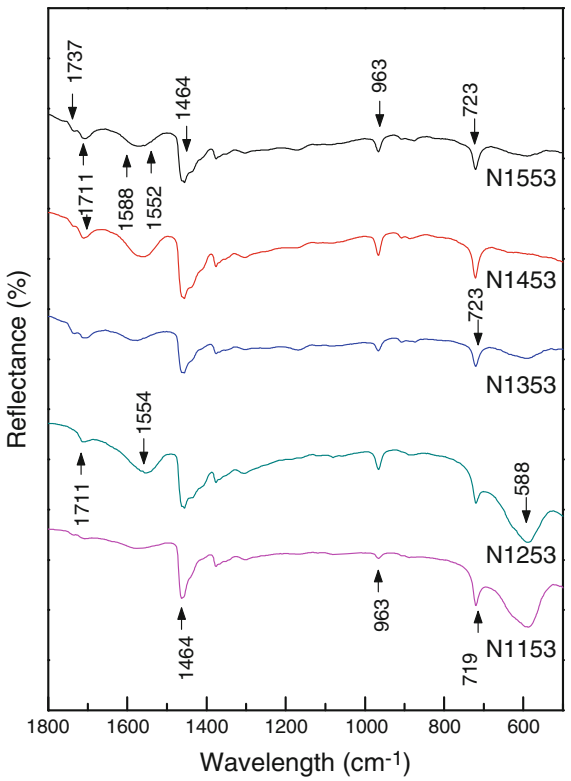

Fig. 4 FTIR spectra of magnetic nanoparticles prepared by thermal decomposition at 320 °C for 30 min in ODE with different molar ratios of metal ion and oleic acid

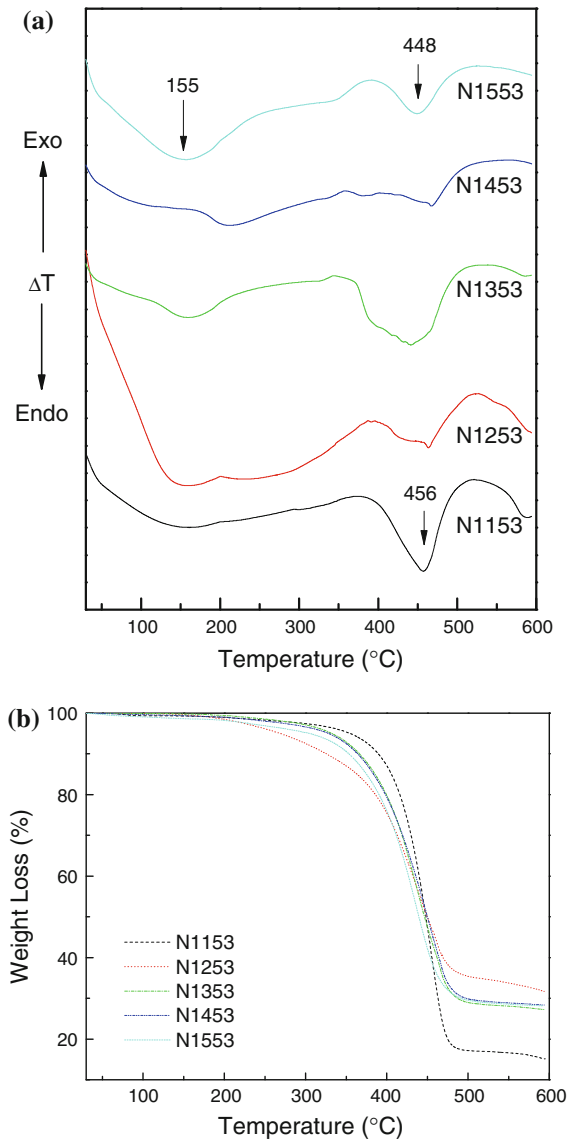

Fig. 5 **a** DTA curves and **b** TGA curves of magnetic nanoparticles prepared by thermal decomposition at 320 °C for 30 min in ODE with different molar ratios of metal ion and oleic acid

prepared SPIONs by different $Fe(NO_3)_3$ and OA amounts as shown in Fig. 5. The SPIONs were washed by precipitation–decantation method for several times to remove the excessive OA before thermal analysis. As seen from DTA curves shown in Fig. 5a, the first transition appeared as a broad endothermic peak around 155 °C, which is assigned to removal of physically absorbed water or ethanol impurities. The second exothermic peak appears at 448–456 °C in all SPIONs samples, corresponding to the dissociation of OA ligand from iron oxide surface. The three-step thermal decomposition behavior of N1553 is shown in Fig. 5b, and described below as a typical example: the first weight loss from 50 to 158 °C is 2.8%, possibly due to removal of physically absorbed water and ethanol residue. Both the second weight loss in the range of 158 to 390 °C and the third weight loss in the range of 390 to 468 °C are due to the removal of coated OA, which is consistent with the DSC endothermic peak at 448 °C. Zobril had proposed two different modes of palmitic acid with SPIONs: the carboxylate head of the inner layer gets attached to the iron oxide surface, and the outer layer palmitic acid interacts with the inner layer surfactant by hydrophobic interaction (Zobril et al. 2008). However, since only a singe significant weight loss happened from 390–468 °C because of combustion of surface-attached OA, there is no evidence to show the interdigitated layer structure of OA coating of our nanoparticles.

Conclusion

The organometallic compounds for thermal decomposition are quite expensive and highly toxic. In this study, we used simple, inexpensive, and environmental-friendly approaches to prepare the metallic surfactants. The yield of the metallic surfactants is 100%, meaning that there is no need to analyze the ion concentration for reaction. In addition, the technique can be performed in one vessel as it does not involve a washing step. We demonstrated a novel synthetic route for non-hydrated FeOl which leads to one-pot reaction for fabrication of SPIONs with tunable size and high monodispersibility. A possible FeOl structure was proposed based on FT-IR analysis. According to the thermal analysis, a complete separation of two endothermic peaks corresponding to nucleation and particle growth was revealed as a predication of high probability of monodispersed SPIONs. TEM shows that various morphologies, such as cubic, triangular, and spherical particles, can be obtained, and diameter of the as-prepared particles can be tuned by varying Fe/OA molar ratios in the starting mixture. Any metal salt (MX) can be used for this process. M can be Cr, Mn, Co, Ni, Cu, Pt, Pd, Au, Ag, Y, Zr, Cd, etc. X can be halide, nitrate, sulfate, etc. Fatty acid is carboxylic acid often with a long, unbranched aliphatic tail (chain), which is either saturated or unsaturated. Also, core–shell structures can be prepared by sequential step-by-step processes.

Acknowledgments This study is supported by Basic Science Research Program through the National Research Foundation of Korea (NRF) funded by the Ministry of Education, Science and Technology (Grant No. 2011-0013675).

References

Bronstein LM, Huang X, Retrum J, Schmucker A, Pink M, Stein BD, Dragnea B (2007) Chem Mater 19(15):3624–3632

Casula MF, Jun YW, Zaziski DJ, Chan EM, Corrias A, Alivisators AP (2006) J Am Chem Soc 128(5):1675–1677

Deng H, Li X, Peng Q, Wang X, Chen J, Li Y (2005) Angew Chem Int Ed Engl 44(18):2782–2785

Feng JH, Zhao J, Hao FH, Chen C, Bhakoo K, Tang HR (2011) NMR-based metabonomic analyses of the effects of ultrasmall superparamagnetic particles of iron oxide (USPIO) on macrophage metabolism. J Nanopart Res 13(5): 2049–2062. doi:10.1007/s11051-010-9959-5

Hyeon T, Lee SS, Park J, Chung Y, Na HB (2001) J Am Chem Soc 123(51):12798–12801

Jeon BS, Cho EJ, Yang HM, Suh JS, Huh YM, Kim JD (2009) Controlled aggregates of magnetite nanoparticles for highly sensitive MR contrast agent. J Nanosci Nanotechnol 9(12):7118–7122. doi:10.1166/jnn.2009.1605

Kim DK, Dobson J (2009) Nanomedicine for targeted drug delivery. J Mater Chem 19(35):6294–6307. doi:10.1039/b902711b

Kwon SG, Piao Y, Park J, Angappane S, Jo Y, Hwang NM, Park JG, Hyeon T (2007) J Am Chem Soc 129(41):12571–12584

Lee JS, Rodriguez-Luccioni HL, Mendez J, Sood AK, Lpez-Berestein G, Rinaldi C, Torres-Lugo M (2011) Hyperthermia induced by magnetic nanoparticles improves the effectiveness of the anticancer drug cis-diamminedichloroplatinum. J Nanosci Nanotechnol 11(5):4153–4157. doi:10.1166/jnn.2011.3821

Li Z, Wei L, Gao MY, Lei H (2005) Adv Mater 17(8):1001–1005

Mahajan SV, Dikerson JH (2007) Nanotechnol 18(32):325605–325611

Park J, An K, Hwang Y, Park JG, Noh HJ, Kim JY, Park JH, Hwang NM, Hyeon T (2004) Nat Mater 3:891–895

Roca AG, Morales MP, O'Grady K, Serna CJ (2006) Nanotechnol 17(11):2783–2788

Shukla N, Liu C, Jones PM, Weller D (2003) J Magn Magn Mater 266(1–2):178–184

Simioni AR, Rodrigues MMA, Primo FL, Morais PC, Tedesco AC (2011) Effect of diode-laser and AC magnetic field of bovine serum albumin nanospheres loaded with phthalocyanine and magnetic particles. J Nanosci Nanotechnol 11(4):3604–3608. doi:10.1166/jnn.2011.3724

Sun S, Zeng H (2002) J Am Chem Soc 124(28):8204–8205

Wang FH, Yoshitake T, Kim DK, Muhammed M, Bjelke O, Kehr J (2003) Determination of conjugation efficiency of antibodies and proteins to the superparamagnetic iron oxide nanoparticles by capillary electrophoresis with laser-induced fluorescence detection. J Nanopart Res 5(1–2): 137–146. doi:10.1023/a:1024428417660

Yeh CH, Hsiao JK, Wang JL, Sheu F (2010) Immunological impact of magnetic nanoparticles (Ferucarbotran) on murine peritoneal macrophages. J Nanopart Res 12(1): 151–160. doi:10.1007/s11051-009-9589-y

Yu WY, Falkner JC, Yavuz CT, Colvin VL (2004) Chem Comm 20:2306–2307

Zobril R, Bakandritsos A, Mashlan M, Tzitzios V, Dallas P, Trapalis C, Petridis D (2008) Nanotechnol 19(9):095602–095610